



# Heat transfer analysis of tangent hyperbolic nanofluid in a ciliated tube with entropy generation

S. Shaheen<sup>1</sup> · K. Maqbool<sup>1</sup> · R. Ellahi<sup>1</sup> · Sadiq M. Sait<sup>2</sup>

Received: 28 November 2020 / Accepted: 11 February 2021 / Published online: 6 March 2021  
 © Akadémiai Kiadó, Budapest, Hungary 2021

## Abstract

In this paper, we analyze the effect of heat transfer on the flow of tangent hyperbolic nanofluid in a ciliated tube (fallopian tube where embryo in blood make the development). This study will be beneficial for the researchers and medical experts in the field of embryology. The nanoparticles are beneficial to remove the cysts from the fallopian tube where development of embryo takes place. To resolves the ciliary flow problems, medical doctors use nanoparticles (drug delivery) that may create a temperature gradient. The heat transfer helps to optimize the energy for which the entropy generation is reduced. Therefore, in this research we discuss the heat transfer effect on tangent hyperbolic nanofluid and entropy generation due to ciliary movement. The governing partial differential equations are solved by HPM and software MATHEMATICA™. Effect of viscoelastic parameter, nanoparticles, cilia length and Brinkman number on the velocity, temperature and entropy generation has been illustrated with the help of graphs. Graphical results show that thermal conductivity of fluid increases by adding nanoparticles. The entropy generation due to nanoparticles will decrease the viscosity near the tube wall and blood through tube will flow with normal pressure.

**Keywords** Heat transfer · Ciliated tube · Tangent hyperbolic fluid · Nanoparticles · Entropy generation

## List of symbols

$V$	Velocity field vector	$\epsilon$	Cilia length
$U, W$	Velocity components in fixed frame	$\rho_f$	Density of fluid
$u, w$	Velocity components in wave frame	$\rho_{nf}$	Density of nanofluid
$R, Z$	Cylindrical coordinates of ciliated tube in fixed frame	$\rho_s$	Density of nanoparticles
$r, z$	Cylindrical coordinates of ciliated tube in wave frame	$\varphi$	Solid volume fraction
$P$	Pressure in fixed frame	$k_{nf}$	Thermal conductivity of nanofluid
$p$	Pressure in wave frame	$k_f$	Thermal conductivity of base fluid
$\tau$	Cauchy stress	$k_s$	Thermal conductivity of solid nanoparticles
$S$	Shear rate	$\alpha$	Eccentricity of elliptical path
$c$	Wave speed	$\eta_\infty$	Infinite shear rate viscosity
$(\rho c_p)_{nf}$	Specific heat capacity of nanofluid	$\eta_0$	Zero shear rate viscosity
$(\rho c_p)_f$	Specific heat capacity of base fluid	$\Gamma$	Time constant
$(\rho c_p)_s$	Specific heat capacity of nanoparticles	$\dot{\gamma}$	Strain rate tensor
		$\pi$	Second order tensor
		$\beta$	Wave number
		$m$	Power law index
		$A_1$	Rivlin–Erickson tensor
		$We$	Weissenberg number
		$\underline{Q}$	Volume flow rate
		$\bar{Q}$	Mean volume flow rate
		$j$	Embedding parameter
		$T$	Temperature profile
		$T_0$	Temperature at the center of the tube
		$T_1$	Temperature at the ciliated wall

✉ K. Maqbool  
 khadija.maqbool@iiu.edu.pk

<sup>1</sup> Department of Mathematics and Statistics, International Islamic University, Islamabad, Pakistan

<sup>2</sup> Center for Communications and IT Research, Research Institute, King Fahd University of Petroleum and Minerals, Dhahran 31261, Saudi Arabia

Re	Reynolds' number
Br	Brinkman number
$N_s$	Entropy generation
Be	Bejan number
$\theta$	Dimensionless temperature

## Introduction

In past few decades, the first law of thermo-dynamics has been used to investigate efficiency of heat transfer. However, in recent years, scientists have observed the entropy generation to analyze the irreversible behavior of matter during heat transfer. It is evident from the literature that many thermal mechanisms show irreversible behavior as irreversibility in a thermal process develops a continuous entropy generation, which demolish the energy of a system. This energy loss is mainly due to heat transfer, viscosity, buoyancy and magnetic field, which occurs in different modes. A detailed discussion on entropy generation for different flow systems was first presented by Bejan [1] who gave the concept of entropy generation; according to him, entropy generation is due to irreversible nature of heat transfer and viscosity effects with the fluid at solid boundaries. Benedetti et al. [2] obtained the numerical results for rate of entropy generation in a tube. Entropy generation in a pipe due to non-Newtonian fluid flow was presented by Pakdemirli et al. [3]. They observed that heat transfer rate and fluid friction increase with the increase in Brinkman number, and entropy number increases. Qasim et al. [4] analyzed the entropy generation in fluid flowing through wavy channel by using Maxwell's thermal conductivity model. Rashidi et al. [5] studied the entropy generation of a nanofluid flow with slip conditions by using effective Prandtl model. Beside these models, different researchers [6–9] presented the convective heat transfer problems with entropy generation in different geometries and observed that entropy generation plays an important role in the flow field.

Heat transfer enhancement in biological fluids is an important area of modern biomechanics and biomedical engineering. Heat regulation is essential for all mammals, human beings and living organism, therefore in modern biomedical engineering [10–14] due to its multifarious applications, has gained lots of importance.

The study of thermodynamics deals with the properties of substances associated with pressure, density, velocity, viscosity, nanofluids and their relationship with energy. Nanofluids are colloidal suspensions of nanosized solid

particles in a liquid, which was first studied by Choi [15]. More recently conducted experiments have shown that nanofluids have substantially higher thermal conductivity than base fluids. Among the many advantages of nanofluids over conventional solid–liquid suspensions, the following are worth mentioning: (i) higher specific surface area, (ii) higher stability of the colloidal suspension, (iii) lower pumping power required to achieve the equivalent heat transfer, (iv) reduced particle clogging compared to conventional colloids, (v) higher level of control of the thermodynamics and transport properties by varying the particle material, (vi) concentration, size, (vii) and shape to name a few Neild et.al [16] extended the corresponding problems of porous medium. There are lot of nanoparticles in blood that are one thousand times smaller than a human hair and the presence of these nanoparticles contribute to severe diseases such as neutropenia, blood cancer, eosinophilia, leukocytosis, etc. In many cases, common methods cannot be used to eliminate these particles. Presently, nanotechnology is being used to separate these nanoparticles from plasma [17].

Ciliary movement has been a special subject in the field of experimental and theoretical biology. The first comprehensive study about cilia was presented by Shack in 1835. It took 20 years to explain the complex structure of cilia motion, and Cilia causes fluid motion due to its cyclic and symmetric movement. To study the fluid motion due to ciliary movement, different approaches have been used in the literature [18–34] such as Lagrange method [21] and particle approach [30] of Lattice Boltzmann method. Cilia are present in respiratory tract, sensory organs, male reproductive system and in fallopian tube. The fallopian tube is lined with the ciliated epithelium where the embryo develops. Blockage of fallopian tube may resist the embryo development which may lead to infertility. The development of embryo takes place in an oviduct which is extended laterally from the uterus and is approximately 10 cm long. The oviducts have two parts: one is wider and longer near the ovaries, and other is narrow and smaller near the uterus which facilitates the transportation of sperm from uterus to egg in the ovaries. The oviducts use the ciliary and peristaltic movement for the development of embryo in ovaries. If oviduct shrinks due to blockage in wider and narrow part, then the embryo development will be badly effected and that may cause abnormalities in fetus.

The drug delivery of nanoparticles to the affected part, like the blocked portion in the oviduct is a safe way. The nanoparticles help to transfer medicine with high efficiency with no

side effects. The drug may damage the fetus growing in the ovary, but the drug delivery by nanoparticles helps to protect the fetus growing in oviduct. There are different routes that can be used to deliver the drugs in human body like through the mouth, skin, nose rectum and uterus. The drug delivery by nanoparticles can be enhanced by the thermal conductivity of convective flow which require energy balance. Also, in bio-heat transfer, we are interested in maximizing the energy which requires the reduction in the entropy generation.

Keeping all above views in mind, this study is designed to see the advantages of nanoparticles for drug delivery in the flow of tangent hyperbolic fluid during the embryo development by reducing the entropy generation. The flow of tangent hyperbolic fluid is observed by the law of conservation of mass and momentum and reduction in entropy generation is measured by the law of conservation of energy. The momentum equation for tangent hyperbolic fluid is modeled by the envelop model approach of ciliary movement. The two-dimensional coupled equations are simplified using the assumption of large oviduct moving peristaltically (long wavelength) and high viscosity of the blood in oviduct (small Reynolds' number). The resulting equations are solved by analytical method HPM and software MATHEMATICA™.

### Mathematical modeling

Consider a two-dimensional flow of Tangent hyperbolic copper nanofluid model in a tube of width  $2h$ . Blood is considered as base fluid, and copper nanoparticles are immersed in blood. Assume that an infinite number of continuously beating cilia are present at the inner walls of tube generating a symplectic metachronal wave which moves towards positive  $z$ -axis with wave speed  $c$  as mentioned in Fig. 1.

Governing equations for an incompressible Tangent hyperbolic nanofluid are defined as follows

$$\nabla \cdot \mathbf{V} = 0, \tag{1}$$

where

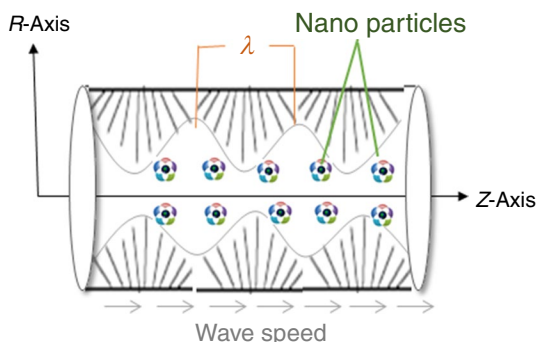


Fig. 1 Geometry of ciliated tube

$$\mathbf{V} = [u, 0, w], \tag{2}$$

and

$$\rho_f \frac{d\mathbf{V}}{dt} = \text{div} \boldsymbol{\tau}, \tag{3}$$

$$(\rho c)_f \frac{dT}{dt} = k_{nf} \nabla^2 T + \text{trace}(\mathbf{S} \cdot \mathbf{L}), \tag{4}$$

where  $\mathbf{V}$  is the velocity components,  $w$  is the axial component of velocity,  $u$  is the radial component of velocity,  $\mathbf{S}$  is the extra stress tensor,  $\frac{d}{dt} = \frac{\partial}{\partial t} + \mathbf{V} \cdot \nabla$  is the total derivative,  $\rho_f$  is the density of nanofluid,  $T$  is the temperature profile and  $L$  is gradient of velocity.

Here, the appropriate stress tensors for the tangent hyperbolic fluid model [35] are as follows

$$\boldsymbol{\tau} = -p\mathbf{I} + \mathbf{S}, \tag{5}$$

$$\mathbf{S} = [(\eta_\infty + (\eta_0 + \eta_\infty) \tanh(\Gamma \dot{\gamma})^m) \dot{\gamma}_i], \tag{6}$$

in which  $\boldsymbol{\tau}$  is the Cauchy stress tensor,  $\eta_0$  represents zero shear rate viscosity,  $\eta_\infty$  is the infinite shear rate viscosity,  $\Gamma$  is time constant and  $m$  shows the power law index.

$$\dot{\gamma} = \sqrt{\frac{1}{2} \boldsymbol{\pi}}, \tag{7}$$

where  $\boldsymbol{\pi} = \text{trace}(\text{grad} \mathbf{V} + \text{grad} \mathbf{V}^T)^2$ ,

where  $\boldsymbol{\pi}$  is second-order tensor. We study the above equation for the case where  $\eta_\infty = 0$  and  $\Gamma \dot{\gamma} < 1$ . The elements of extra stress tensor can be written as

$$\dot{\gamma}_i = \mathbf{L} + \mathbf{L}^T, \tag{8}$$

$$\bar{\tau} = \eta_0 ((\Gamma \dot{\gamma})^m) \dot{\gamma}_i = \eta_0 (1 + \Gamma \dot{\gamma} - 1)^m \dot{\gamma}_i = \eta_0 (1 + m(\Gamma \dot{\gamma} - 1)) \dot{\gamma}_i \tag{9}$$

where thermal conductivity of nanofluid is defined as

$$\rho_{nf} = (1 - \varphi) \rho_f + \varphi \rho_s, \tag{10a}$$

$$\eta_{nf} = \frac{\eta_f}{(1 - \varphi)^{2.5}}, \tag{10b}$$

$$(\rho c_p)_{nf} = (1 - \varphi) (\rho c_p)_f + \varphi (\rho c_p)_s, \tag{10c}$$

$$\alpha_{nf} = \frac{k_{nf}}{(\rho c_p)_{nf}}, \tag{10d}$$

$$k_{nf} = k_f \left( \frac{k_s + 2k_f - 2\varphi(k_f - k_s)}{k_s + 2k_f + 2\varphi(k_f - k_s)} \right) \tag{10d}$$

where  $k_{nf}$  is the thermal conductivity of nanofluid,  $k_f$  is the thermal conductivity of base fluid,  $k_s$  is the thermal conductivity of solid nanoparticles and  $\varphi$  is the solid volume fraction. The Mathematical model for geometry of cilia tips in the wave frame is

$$h = 1 + \epsilon \cos 2\pi z, \tag{11a}$$

$$w(h) = -1 - 2\pi\epsilon\alpha\beta \cos 2\pi z. \tag{11b}$$

where  $\epsilon$  is the cilia length parameter,  $\alpha$  is the eccentricity of elliptic wave and  $\beta$  is the wave number.

The governing equations of motion of tangent hyperbolic fluid model in a tube are specified as follows.

$$\frac{\partial u}{\partial r} + \frac{u}{r} + \frac{\partial w}{\partial z} = 0, \tag{12}$$

$$\rho_f \left[ u \frac{\partial w}{\partial r} + w \frac{\partial w}{\partial z} \right] = -\frac{\partial p}{\partial z} + \frac{1}{r} \frac{\partial}{\partial z} (rS_{rz}) + \frac{\partial S_{zz}}{\partial z} \tag{13}$$

$$\rho_f \left[ u \frac{\partial u}{\partial r} + w \frac{\partial u}{\partial z} \right] = -\frac{\partial p}{\partial r} + \frac{1}{r} \frac{\partial}{\partial r} (rS_{rr}) + \frac{\partial S_{rz}}{\partial z}, \tag{14}$$

$$(\rho c)_f \left[ u \frac{\partial T}{\partial r} + w \frac{\partial T}{\partial z} \right] = k_{nf} \left( \frac{1}{r} \frac{\partial}{\partial r} \left( r \frac{\partial T}{\partial r} \right) + \frac{\partial^2 T}{\partial z^2} \right) + S_{rz} \frac{\partial w}{\partial r}. \tag{15}$$

where  $\rho_f$  is the fluid density,  $u$  and  $w$  are the radial and axial components of velocity,  $c$  is the wave speed and  $\eta_f$  is the apparent viscosity of fluid.

The following non-dimensional parameters can be introduced for further analysis.

$$\begin{aligned} z^* &= \frac{z}{\lambda}, r^* = \frac{r}{a}, u^* = \frac{u}{\beta c}, w^* = \frac{w}{c}, h^* = \frac{h}{a}, \\ p^* &= \frac{a\beta}{c\eta_f} p, \beta = \frac{a}{\lambda}, S_{ij}^* = \frac{a}{\eta_f c} S_{ij}, \lambda_1 = \frac{c\lambda_1}{a}, \\ \text{Re} &= \frac{\rho a c}{\eta_f}, \text{We} = \frac{\Gamma c}{a}, \alpha_f = \frac{k}{(\rho c)_f}, \theta = \frac{T - T_0}{T_0}, \\ \text{Br} &= \frac{a^2 \eta_f}{k_f T_0}, \text{Pr} = \frac{\eta_f c_p}{k_f}, \text{Ec} = \frac{c^2}{c_p T_0}. \end{aligned} \tag{16}$$

where  $\lambda, a, c$  symbolize the wavelength, width of velocity and wave speed, respectively, Re is the Reynolds' numbers,

$\beta$  is the wave number and  $D_a$  is the Darcy's number. In terms of dimensionless parameters, the momentum equations and shear stresses are

$$\frac{\partial u}{\partial r} + \frac{u}{r} + \frac{\partial w}{\partial z} = 0, \tag{17}$$

$$\text{Re}\beta \left[ u \frac{\partial w}{\partial r} + w \frac{\partial w}{\partial z} \right] = -\frac{\partial p}{\partial z} + \frac{1}{r} \frac{\partial}{\partial z} (rS_{rz}) + \beta \frac{\partial S_{zz}}{\partial z} \tag{18}$$

$$\text{Re}\beta^2 \left[ u \frac{\partial u}{\partial r} + w \frac{\partial u}{\partial z} \right] = -\frac{\partial p}{\partial r} + \frac{\beta}{r} \frac{\partial}{\partial r} (rS_{rr}) + \beta^2 \frac{\partial S_{rz}}{\partial z} - \beta \frac{\partial S_{\theta\theta}}{\partial z}, \tag{19}$$

$$\beta(\rho c)_f \left[ u \frac{\partial \theta}{\partial r} + w \frac{\partial \theta}{\partial z} \right] = k_{nf} \left( \frac{1}{r} \frac{\partial}{\partial r} \left( r \frac{\partial \theta}{\partial r} \right) + \beta^2 \frac{\partial^2 \theta}{\partial z^2} \right) + S_{rz} \frac{\partial w}{\partial r}, \tag{20}$$

$$S_{rz} = \left( 1 + m \left( \text{We} \frac{\partial w}{\partial r} - 1 \right) \right) \frac{\partial w}{\partial r}. \tag{21}$$

Using long wavelength approximation ( $\beta \rightarrow 0$ ) given in [36], the governing equations and boundary conditions are as follows

$$\frac{\partial p}{\partial z} = (1 - m) \frac{1}{r} \frac{\partial}{\partial r} \left( r \frac{\partial w}{\partial r} \right) + m \text{We} \frac{1}{r} \frac{\partial}{\partial r} \left( r \left( \frac{\partial w}{\partial r} \right)^2 \right) \tag{22}$$

$$-\frac{\partial p}{\partial r} = 0, \tag{23}$$

$$\frac{k_{nf}}{k_f} \frac{1}{r} \frac{\partial}{\partial r} \left( r \frac{\partial \theta}{\partial r} \right) = -\text{Br} \frac{\eta_{nf}}{\eta_f} \left( 1 + m \left( \text{We} \frac{\partial w}{\partial r} - 1 \right) \right) \left( \frac{\partial w}{\partial r} \right)^2. \tag{24}$$

$$\frac{\partial w}{\partial r} = 0, \frac{\partial \theta}{\partial r} = 0 \text{ at } r = 0, \tag{25a}$$

$$w = w(h), \theta = 0 \text{ at } r = h. \tag{25b}$$

Integration of Eq. (17) over the tube width is given as:

$$\int_0^h \left[ \frac{1}{r} \frac{\partial (ru)}{\partial r} + \frac{\partial w}{\partial z} \right] r dr = 0, \tag{26}$$

$$hu(h) + \frac{1}{2} \frac{\partial q}{\partial z} - h \frac{\partial h}{\partial z} w(h) = 0, \tag{27}$$

where  $q = 2 \int_0^h r w dr$

Equation (27) can be written as

$$\frac{\partial q}{\partial z} = 2h \left( \frac{\partial h}{\partial z} w(h) - u(h) \right), \quad (28)$$

The relation between  $q$  and dimensionless volume flow rate  $Q$  is given by

$$Q = 2 \int_0^h RWdR = 2 \int_0^h (w+1)rdr = q + h^2, \quad (29)$$

The mean volume flow rate for the time period  $T = \frac{\lambda}{c}$  is

$$\bar{Q} = \frac{1}{T} \int_0^T Q dt^* = q + 1 + \frac{\epsilon^2}{2}, \quad (30)$$

where  $\lambda$  is the wavelength of metachronal wave,  $c$  is the wave speed and  $t^*$  is the mean average time.

## Solution of the problem

To obtain the solution of governing equations, we use homotopy perturbation method [37] which is described as follows

$$H(j, w) = (1-j)(\mathcal{L}(w) - \mathcal{L}(w_0)) + j \left( \mathcal{L}(w) - \frac{1}{(1-\varphi)^{2.5}} \frac{\partial p}{\partial z} + \frac{1}{r} \frac{\partial}{\partial r} \left( rmWe \left( \frac{\partial w}{\partial r} \right)^2 \right) \right), \quad (31)$$

$$H(j, \theta) = (1-j)(\mathcal{L}(\theta) - \mathcal{L}(\theta_0)) + j \left( \mathcal{L}(\theta) - \frac{Br}{(1-\varphi)^{2.5}} \frac{k_f}{k_{nf}} \left( 1 + m \left( We \frac{\partial w}{\partial r} - 1 \right) \right) \left( \frac{\partial \theta}{\partial r} \right)^2 \right), \quad (32)$$

The linear operator and initial guesses are chosen as

$$\mathcal{L}(w) = \frac{1}{r} \frac{\partial}{\partial r} \left( r(1-m) \frac{\partial}{\partial r} \right), \quad (33)$$

$$\mathcal{L}(\theta) = \frac{1}{r} \frac{\partial}{\partial r} \left( r \frac{\partial}{\partial r} \right). \quad (34)$$

$$w_0 = \frac{(1-\varphi)^{2.5}}{4(1-m)} \frac{dp_0}{dz} (r^2 - h^2) + w(h), \quad (35)$$

$$\theta_0 = \frac{r^2 - h^2}{4}. \quad (36)$$

According to homotopy perturbation method,

$$w = w_0 + jw_1 + j^2w_2 \dots, \quad (37a)$$

$$\theta = \theta_0 + j\theta_1 + j^2\theta_2 \dots, \quad (37b)$$

$$p = \theta_0 + jp_1 + j^2p_2 \dots, \quad (37c)$$

where  $j \in [0,1]$  is the homotopy perturbation parameter and  $j = 0$  gives initial guess and  $j = 1$  gives the final solution. With the help of Eqs. (31)–(37), the second-order solution for the velocity and temperature profile are given as follows

$$w = w(h) + A_1(r^2 - h^2) + A_2(r^3 - h^3), \quad (38)$$

And temperature profile can be found in following manner

$$\theta = \frac{1}{(1-\varphi)^{2.5}} \frac{k_f}{k_{nf}} \left( \frac{A_3}{16} (r^4 - h^4) + \frac{A_4}{25} (r^5 - h^5) + \frac{A_5}{36} (r^6 - h^6) \right) + \frac{1}{(1-\varphi)^{2.5}} \frac{k_f}{k_{nf}} \left( \frac{A_6}{49} (r^7 - h^7) + \frac{A_7}{64} (r^8 - h^8) \right). \quad (39)$$

Integrating Eq. (27) using software MATHEMATICA™ calculating pressure gradient as

$$\frac{dp}{dz} = \frac{-A_9 \pm \sqrt{A_9^2 - 4A_8A_{10}}}{2A_8}. \quad (40)$$

## Entropy generation

Entropy generation can be written as

$$S'''_{\text{gen}} = \frac{k_f}{T_\infty^2} \left( \left( \frac{\partial T}{\partial r} \right)^2 + \left( \frac{\partial T}{\partial z} \right)^2 \right) + \frac{1}{T_0} \tau_{\text{zr}} \frac{\partial w}{\partial r}. \quad (41)$$

Dimensionless form of Entropy generation can be written as

$$N_S = \frac{S'''_{\text{gen}}}{S'''_G} = \left( \frac{\partial \theta}{\partial r} \right)^2 + Br\Lambda \left( 1 + m \left( We \frac{\partial w}{\partial r} - 1 \right) \right) \left( \frac{\partial w}{\partial r} \right)^2 \quad (42)$$

$$S'''_G = \frac{k_f T_0^2}{-2}, \Lambda = \frac{\theta_0}{T_0}. \quad (43)$$

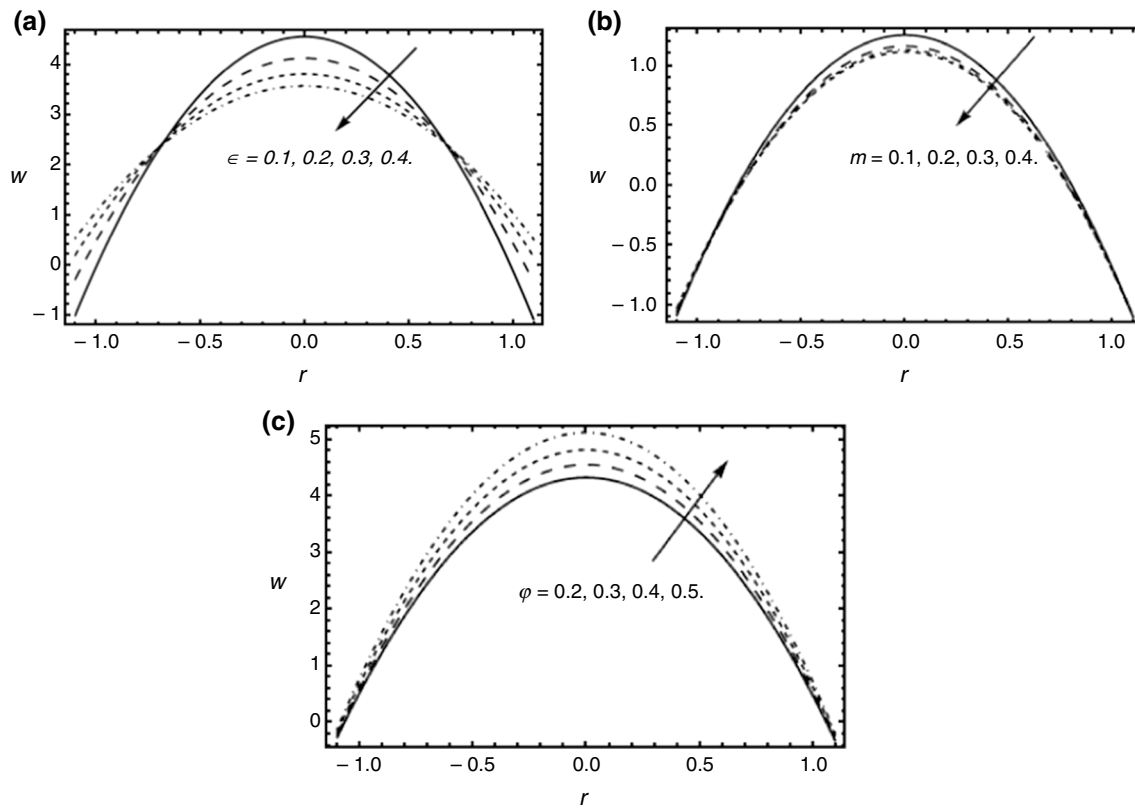


**Fig. 2** a–c The effect of cilia length parameter  $\epsilon$ , power law index  $m$  and nanoparticles volume fraction  $\phi$  fraction on axial velocity.

## Results and discussion

In this section, the graphical results show the effects of different parameters of interest. The cilia-induced flow of a Tangent hyperbolic nanofluid in circular tube is investigated. The effect of emerging parameters for the entropy generation, and stream functions are observed by keeping all other parameters fixed as suggested in Ref. [38]

Axial velocity for different values of, cilia length  $\epsilon$ , power law index  $m$  and nanoparticle volume fraction of the fluid  $\phi$  are observed in Fig. 2a–c. In Fig. 2a, the velocity of fluid decreases by increasing cilia length parameter as increase in cilia length resist the fluid flow at the centre of tube. Figure 2b shows that velocity of fluid decreases by increasing

power law index  $m$  because for increasing  $m$  fluid behaves like a shear thickening fluid which causes the decrease in velocity of fluid. Figure 2c shows that velocity increases by increasing nanoparticle volume fraction of the fluid because when nanoparticles are more in fluid, due to their smaller size they will move with high speed.

Temperature profile for different values of nanoparticle volume fraction of the fluid  $\phi$ , power law index  $m$  and Brinkman number  $Br$  is observed in Fig. 3a–c. It can be seen that temperature is maximum at the centre of tube and minimum at the ciliated walls where it is effected by ciliated walls. Figure 3a illustrates that by increasing nanoparticle volume fraction of the fluid  $\phi$ , temperature profile decreases. Graphical results show that nanofluids can increase heat transfer

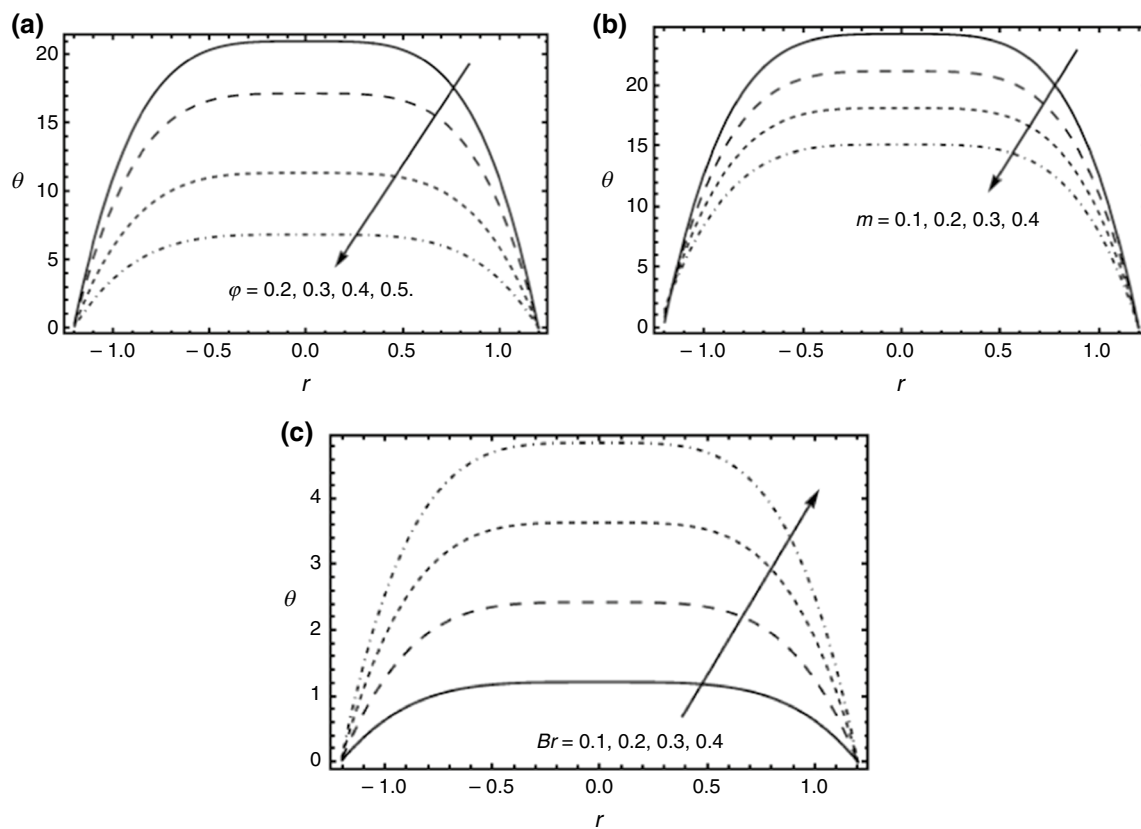


**Fig. 3** a–c The effect of nanoparticles volume fraction  $\phi$ , power law index  $m$  and Brinkman number  $Br$  on temperature profile

rate by decreasing the wall temperature. Also, Fig. 3b shows that by increasing power law index  $m$  temperature profile decreases. Brinkman number is the ratio of viscous heat generation to external heating. So by increasing Brinkman number viscous heat generation will increase as compared to external heating; therefore, temperature will increase.

In Fig. 4a–c, entropy generation for different values of nanoparticle volume fraction of the fluid  $\phi$ , power law index  $m$  and Brinkman number  $Br$  are observed. It can be depicted from the graphs that entropy generation is maximum at the ciliated walls and minimum at the centre of tube.

Bejan number for different values of nanofluid volume fraction  $\phi$ , power law index  $m$  and Brinckman number  $Br$  is observed in Fig. 5a–c. Since due to less temperature

gradient at the centre of tube, heat transfer is small and very less resistance occurs at center due to which Bejan number decreases at center of tube and has maximum values at boundaries. Furthermore, by increasing  $\phi$ , Bejan number decreases while by increasing Brinkman number  $Br$  Bejan number increases.

Figure 6a, b shows the comparison of symplectic and antiplectic wave patterns for different values of nanoparticles volume fraction  $\phi$  and power law index  $m$ . It can be seen that symplectic wave pattern is more efficient than antiplectic wave pattern for increasing values of nanoparticles volume fraction  $\phi$  and power law index  $m$ .

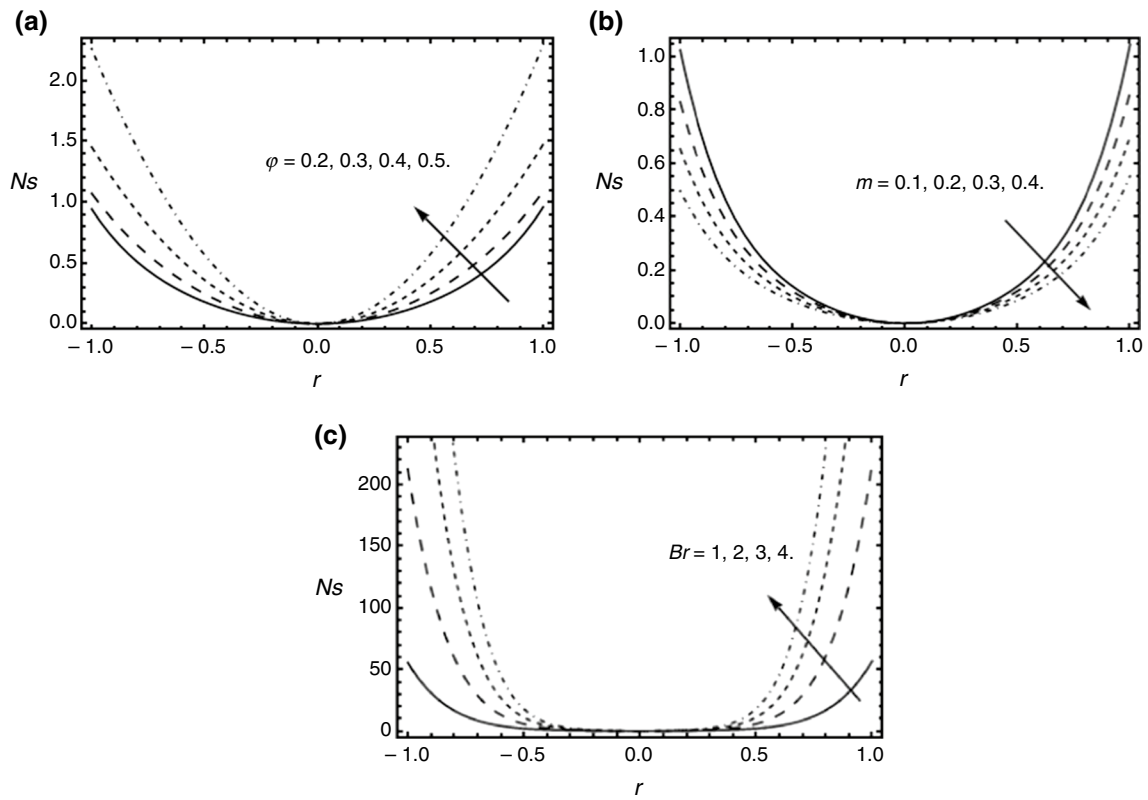


Fig. 4 a–c The effect of nanoparticles volume fraction  $\phi$ , Brinkman number  $Br$  and power law index  $m$  on entropy generation

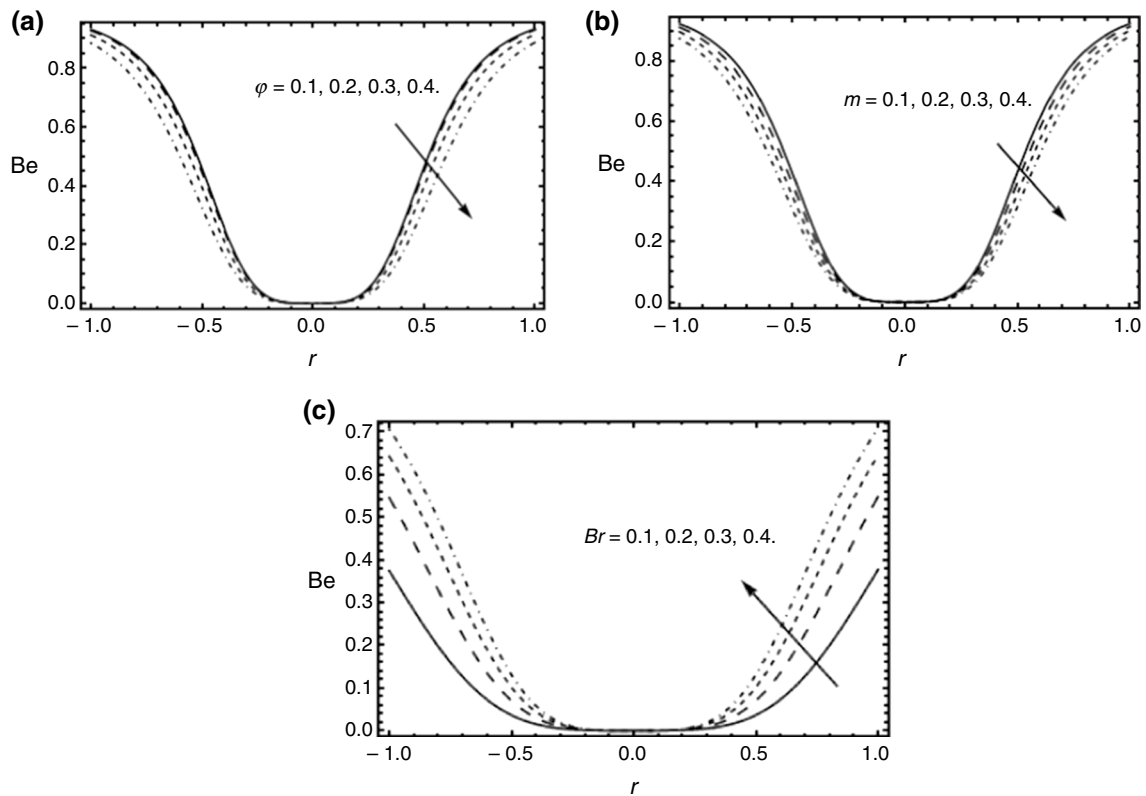
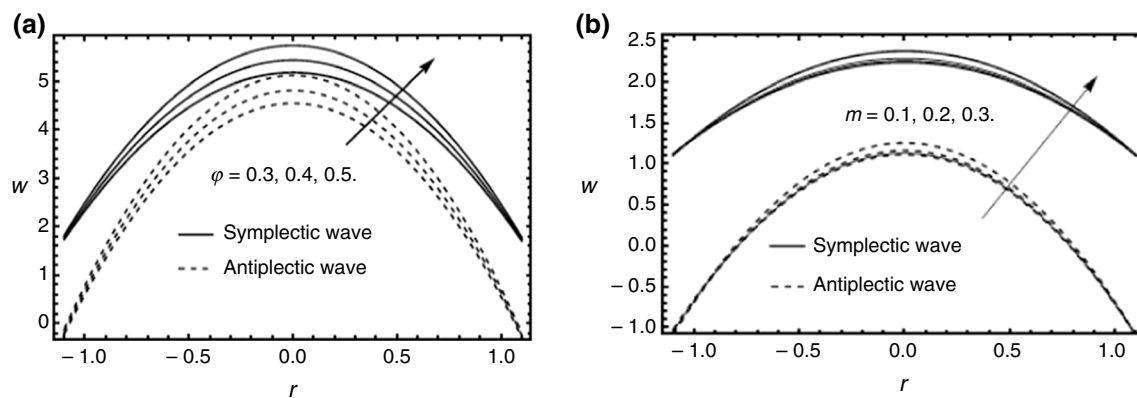


Fig. 5 a–c The effect of nanoparticles volume fraction  $\phi$ , power law index  $m$  and Brinkman number  $Br$  on Bejan number





**Fig. 6** a, b Comparison of symplectic and antiplectic wave for different values of nanoparticles volume fraction  $\varphi$  and power law index  $m$

## Conclusions

In this study, we have developed a mathematical model of velocity and temperature profile in the presence of nanoparticles in base fluids. Fluid motion is produced by the periodic beating of ciliated surface. The surface of cilia is considered as a continuous envelop whose motion is found by the metachronal wave formed by the coordinated cilia. The boundary conditions are defined at mean radius of cylinder; therefore, horizontal and vertical velocities are defined at the mean radius ( $r = a$ ). The governing differential equations involve the parameter depend upon, volume fractions of nanoparticles. The differential equations are solved by homotopy perturbation method (HPM).

- This study helps the treatment of heart patient, when clots on blockages have been observed in blood, nanoparticles will help to remove the clot and blockages from blood.
- Axial velocity of the fluid increases by inserting nanoparticles.
- Thermal conductivity of fluid increases by adding nanoparticles.
- The entropy generation due to nanoparticles will decrease the viscosity on the wall so of tube and blood will flow with less/normal pressure.

## References

1. Bejan A. A study of entropy generation in fundamental convective heat transfer. *J Heat Transf*. 1979;101:718–25.
2. Benedetti P, Sciubba E. Numerical calculation of the local rate of entropy generation in the flow around a heated finned-tube. *ASME*. 1993;30:81–91.
3. Pakdemirli M, Yilbas BS. Entropy generation in a pipe due to non-Newtonian fluid flow: constant viscosity case. *Sadhana*. 2006;31(1):21–9.
4. Qasim M, Hayat Khan Z, Khan I, Al-Mdallal QM. Analysis of entropy generation in flow of methanol-based nanofluid in a sinusoidal wavy channel. *Entropy*. 2017. <https://doi.org/10.3390/e19100490>.
5. Rashidi MM, Abbas MA. Effect of slip conditions and entropy generation analysis with an effective Prandtl number model on a nanofluid flow through a stretching sheet. *Entropy*. 2017. <https://doi.org/10.3390/e19080414>.
6. Oztop HF, Al-Salem K. A review on entropy generation in natural and mixed convection heat transfer for energy systems. *Renew Sustain Ener Rev*. 2012;16(1):911–31.
7. Selimefendigil F, Öztot HF. MHD mixed convection and entropy generation of power law fluids in a cavity with a partial heater under the effect of a rotating cylinder. *Int J Heat Mass Transf*. 2016;98:40–51.
8. Selimefendigil F, Öztot HF, Abu-Hamdeh N. Natural convection and entropy generation in nanofluid filled entrapped trapezoidal cavities under the influence of magnetic field. *Entropy*. 2016. <https://doi.org/10.3390/e18020043>.
9. Gibanov NS, Sheremet MA, Oztot HF, Al-Salem K. MHD natural convection and entropy generation in an open cavity having different horizontal porous blocks saturated with a ferrofluid. *J Magn Magn Mater*. 2018;452:193–204.
10. Zeeshan A, Bhatti MM, Muhammad T, Zhang L. Magnetized peristaltic particle–fluid propulsion with Hall and ion slip effects through a permeable channel. *Physica A*. 2020. <https://doi.org/10.1016/j.physa.2019.123999>.
11. Riaz A, Zeeshan A, Bhatti MM, Ellahi R. Peristaltic propulsion of Jeffrey nano-liquid and heat transfer through a symmetrical duct with moving walls in a porous medium. *Physica A*. 2020. <https://doi.org/10.1016/j.physa.2019.123788>.
12. Alolaiyan H, Riaz A, Razaq A, Saleem N, Zeeshan A, Bhatti MM. Effects of double diffusion convection on third grade nanofluid through a curved compliant peristaltic channel. *Coatings*. 2020. <https://doi.org/10.3390/coatings10020154>.
13. Ijaz N, Riaz A, Zeeshan A, Ellahi R, Sait SM. Buoyancy driven flow with gas-liquid coatings of peristaltic bubbly flow in elastic walls. *Coatings*. 2020. <https://doi.org/10.3390/coatings10020115>.
14. Abd-Elaziz EM, Marin M, Othman MI. On the effect of Thomson and initial stress in a thermo-porous elastic solid under GN electromagnetic theory. *Symmetry*. 2019. <https://doi.org/10.3390/sym11030413>.

15. Choi SU, Eastman JA. Enhancing thermal conductivity of fluids with nanoparticles. Lemont: Argonne National Lab; 1995.
16. Niold DA, Kuznetsov AV. The Cheng–Minkowycz problem for natural convective boundary-layer flow in a porous medium saturated by a nanofluid. *Int J Heat Mass Transf.* 2009;52:5792–5.
17. Ibsen S, Sonnenberg A, Schutt C, Mukthavaram R, Yeh Y, Ortac I, Manouchehri S, Kesari S, Esener S, Heller MJ. Recovery of drug delivery nanoparticles from human plasma using an electrokinetic platform technology. *Small.* 2015;11(38):5088–96.
18. Sleight MA, Blake JR, Liron N. The propulsion of mucus by cilia. *Am Rev Resp Dis.* 1988;137(3):726–41.
19. Brennen C, Winet H. Fluid mechanics of propulsion by cilia and flagella. *Ann Rev Fluid Mech.* 1977;9(1):339–98.
20. Sanderson MJ, Sleight MA. Ciliary activity of cultured rabbit tracheal epithelium: beat pattern and metachrony. *J Cell Sci.* 1981;47(1):331–47.
21. Vlase S, Marin M, Öchsner A, Scutaru ML. Motion equation for a flexible one-dimensional element used in the dynamical analysis of a multibody system. *Contin Mech Thermodyn.* 2019;31(3):715–24.
22. Blake J. A model for the micro-structure in ciliated organisms. *J Fluid Mech.* 1972;55(1):1–23.
23. Ross SM, Corrsin S. Results of an analytical model of mucociliary pumping. *J Appl Phys.* 1974;37(3):333–40.
24. Zadkhash M, Toghraie D, Karimipour A. Developing a new correlation to estimate the thermal conductivity of MWCNT-CuO/water hybrid nanofluid via an experimental investigation. *J Therm Anal Calorim.* 2017;129(2):859–67.
25. Varzaneh AA, Toghraie D, Karimipour A. Comprehensive simulation of nanofluid flow and heat transfer in straight ribbed microtube using single-phase and two-phase models for choosing the best conditions. *J Therm Anal Calorim.* 2020;139(1):701–20.
26. Rashidi S, Javadi P, Esfahani JA. Second law of thermodynamics analysis for nanofluid turbulent flow inside a solar heater with the ribbed absorber plate. *J Therm Anal Calorim.* 2019;135(1):551–63.
27. Maleki H, Safaei MR, Togun H, Dahari M. Heat transfer and fluid flow of pseudo-plastic nanofluid over a moving permeable plate with viscous dissipation and heat absorption/generation. *J Therm Anal Calorim.* 2019;135:1643–54.
28. Szilágyi IM, Santala E, Heikkilä M, Kemell M, Nikitin T, Khrichtchev L, Räsänen M, Ritala M, Leskelä M. Thermal study on electrospun polyvinylpyrrolidone/ammonium metatungstate nanofibers: optimising the annealing conditions for obtaining WO<sub>3</sub> nanofibers. *J Therm Anal Calorim.* 2011. <https://doi.org/10.1007/s10973-011-1631-5>.
29. Bagherzadeh SA, Jalali E, Sarafranz MM, Akbari OA, Karimipour A, Goodarzi M, Bach QV. Effects of magnetic field on micro cross jet injection of dispersed nanoparticles in a microchannel. *Int J Numer Methods H.* 2019;30:2683–704.
30. Hosseini R, Rashidi S, Esfahani JA. A lattice Boltzmann method to simulate combined radiation–force convection heat transfer mode. *J Braz Soc Mech Sci Eng.* 2017;39:3695–706.
31. Hajatzadeh Pordanjani A, Aghakhani S, Karimipour A, Afrand M, Goodarzi M. Investigation of free convection heat transfer and entropy generation of nanofluid flow inside a cavity affected by magnetic field and thermal radiation. *J Therm Anal Calorim.* 2019;137:997–1019.
32. Tian Z, Arasteh H, Parsian A, Karimipour A, Safaei MR, Nguyen TK. Estimate the shear rate & apparent viscosity of multi-phased non-Newtonian hybrid nanofluids via new developed support vector machine method coupled with sensitivity analysis. *Physica A.* 2019. <https://doi.org/10.1016/j.physa.2019.122456>.
33. Shamsabadi H, Rashidi S, Esfahani JA. Entropy generation analysis for nanofluid flow inside a duct equipped with porous baffles. *J Therm Anal Calorim.* 2019;135:1009–19.
34. Peng Y, Zahedidastjerdi A, Abdollahi A, Amindoust A, Bahrami M, Karimipour A, Goodarzi M. Investigation of energy performance in a U-shaped evacuated solar tube collector using oxide added nanoparticles through the emitter, absorber and transmittal environments via discrete ordinates radiation method. *J Therm Anal Calorim.* 2020;139:2623–31.
35. Jyothi S, Reddy MS, Gangavathi P. Hyperbolic tangent fluid flow through a porous medium in an inclined channel with peristalsis. *Int J Adv Sci Res Manag.* 2016;1(4):113–21.
36. Maqbool K, Shaheen S, Mann AB. Exact solution of cilia induced flow of a Jeffrey fluid in an inclined tube. *Springer Plus.* 2016;5(1):1–6.
37. Wazwaz AM. Partial differential equations and solitary waves theory. Cham: Springer Science & Business Media; 2010.
38. Saleem N, Munawar S. Entropy analysis in cilia driven pumping flow of hyperbolic tangent fluid with magnetic field effects. *Fluid Dyn Res.* 2020. <https://doi.org/10.1088/1873-7005/ab724b>.

**Publisher's Note** Springer Nature remains neutral with regard to jurisdictional claims in published maps and institutional affiliations.